Journal of Crystal Growth 310 (2008) 3062–3066

Contents lists available at ScienceDirect

Journal of Crystal Growth

journal homepage: www.elsevier.com/locate/jcrysgro

Properties and characterization of Cu_3SbS_3 nanowires synthesized by solvothermal route

M.X. Wang [a,b], G.H. Yue [c,*], X.Y. Fan [a], P.X. Yan [a,*]

[a] School of Physical Science & Technology, Lanzhou University, Lanzhou 730000, China
[b] Lanzhou Polytechnical College, Lanzhou 730050, China
[c] Department of Materials Science and Engineering, Xiamen University, Xiamen 361005, China

ARTICLE INFO

Article history:
Received 22 November 2007
Received in revised form
10 March 2008
Accepted 10 March 2008
Communicated by B.A. Korgel
Available online 12 March 2008

PACS:
61.46.Hk
78.67.Bf
81.07.Vb

Keywords:
A1. Single-crystalline
A2. Solvothermal route
B1. Cu_3SbS_3
B1. Nanowires

ABSTRACT

Cu_3SbS_3 nanowires were successfully obtained through mild solvothermal routes at 150, 160 and 170 °C for 24 h, based on reactions between CuCl, $SbCl_3$ and elemental sulfur in ethylenediamine. The phase, morphology and purity of products have been investigated using X-ray diffraction, transmission electron microscope and X-ray photoelectron spectra methods, respectively. Ethylenediamine played an important role in the formation of the ternary sulfides. A mechanism is proposed to explain the chemical reactions.

1. Introduction

Multiple chalcogenide materials are of considerable interest as the promising semiconductor for electro-optic devices [1–4], thermoelectric devices and optical recording media [5,6]. Being the promising materials with potential applications, they can be prepared in a variety of ways [7,8]. However, there are limited studies of reaction mechanisms, which are very important for the design of new reaction pathways and the control of reaction conditions. On the other hand, the traditional routes to synthesize multiple-component chalcogenides always involve the preparation of precursors, and (or) high temperature, and (or) high pressure, and (or) inert atmosphere protection, and it is difficult to obtain nanocrystalline materials under such conditions. Meanwhile, it is reported that size and (or) dimension reduction always results in substantial alteration of chemical, mechanical, electrical, electro-optical and magnetic properties [9–11]. So it is worthwhile to study the reaction mechanisms and investigate the preparation of the multiple-component chalcogenide nanomaterials, due to their interesting properties and potential applications.

Furthermore, one of the goals of modern solid-state chemistry is to prepare new advanced materials at relatively low temperature [12]. Our approach for this problem concentrates on the preparation of novel nanomaterials by a simple solvothermal routes. In this route, the reactions proceed in the intermediate thermal region (100–300 °C), the reaction velocity is easily controlled, and the organic solvents generally have low viscosity [13], this is favorable for the formation of crystal and the control of crystallite sizes. So the solvothermal methods are suitable for the preparation of novel nanomaterials with good crystallinity [14]. Our Groups have prepared many nanocrystals based on different solvothermal routes [15–17]. In this study, we extended the solvothermal method to the preparation of the ternary metal sulfides. Nanocrystalline Cu_3SbS_3 was successfully synthesized in ethylenediamine based on the reactions between CuCl, $SbCl_3$ and elemental sulfur. Here, being a reaction medium and reducing ligand, ethylenediamine directly took part in the reaction processes and controlled the homogeneous formation of nanocrystalline Cu_3SbS_3.

2. Experiment

Analytically pure CuCl (5.04 mmol), $SbCl_3$(5.04 mmol) and sulfur powder (12.5 m mol) were added into a Teflon-lined

* Corresponding authors. Tel./fax: +86 592 2180155 (G.H. Yue), Tel.: +86 931 8912719; fax: +86 931 8913554 (P.X. Yan).
E-mail addresses: yuegh@126.com (G.H. Yue), pxyan@lzu.edu.cn (P.X. Yan).

0022-0248/$ - see front matter © 2008 Elsevier B.V. All rights reserved.
doi:10.1016/j.jcrysgro.2008.03.012

stainless-steel autoclave which was subsequently filled with anhydrous ethylenediamine up to 90% of its capacity (50 ml). The autoclave was maintained constantly at 150, 160 and 170 °C for 24 h, afterwards cooled to room temperature naturally. The precipitate was filtered, washed with absolute ethanol and distilled water, respectively, and then dried in vacuum at 70 °C for 4 h. A black product was obtained. The final products were collected for characterization.

The phase purity of the as-synthesized product was examined by X-ray diffraction (XRD) using Rigaku Rint-2000 diffractometer with monochromatized Cu Kα radiation ($\lambda = 0.15405$ nm). The nano/microstructure of the Cu_3SbS_3 product was further observed by transmission electron microscope (TEM) and field-emission scanning electron microscope (FESEM), which were performed on a Hitachi Model H-800 (200 kV) and a field-emission microscope (S-4800, 15 kV), respectively. The high-resolution transmission electron microscope (HRTEM) image and the corresponding SAED pattern were taken with a JEOL-2010 TEM with an accelerating voltage of 200 kV. Purity and composition of the product was detected by X-ray photoelectron spectra (XPS) on an ESCALab MKII instrument with MgKα radiation as the exciting source.

3. Results and discussion

The phase purity of the product was examined by XRD, the operation voltage and current were maintained at 40 kV and 40 mA, respectively. In Fig. 1, it can be found that the sample prepared at 160 °C (Fig. 1(b) have many peaks attributed to the single-orthorhombic phase of Cu_3SbS_3, such as the strongest peak of (2 2 2), the stronger peak of (2 0 0), (3 2 1), (4 1 1), (4 4 0) and (6 3 1), and the weak peak of (1 1 0), (4 0 0), (4 3 1), etc. The cell constants are calculated as follows: $a = 6.05$, $b = 14.6$, and $c = 3.81$ Å. Similarly, other samples that we prepared with different temperature (150 and 170 °C) were also identified as the same phase, but the crystal growth direction was shifted with the temperature increasing.

FESEM images of the as-prepared product are shown in Fig. 2(a and b), which reveals that it consists of a large quantity of uniform nanowires. The length of Cu_3SbS_3 nanowires have a typical range of several hundred nanometers to several micrometers. Seen from Fig. 2(b), the diameter of the Cu_3SbS_3 nanowires is ~30 nm. Fig. 2(c) shows the TEM image of Cu_3SbS_3 nanowires, which cross and overlap or reunite with each other.

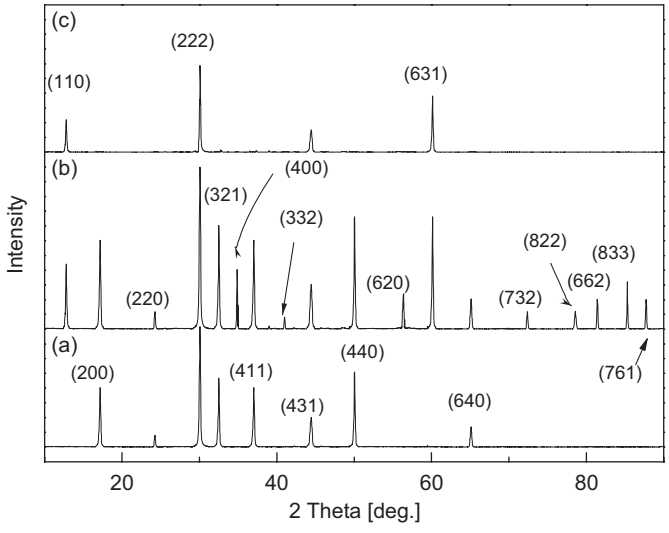

Fig. 1. XRD patterns of the as-prepared nanocrystalline Cu_3SbS_3.

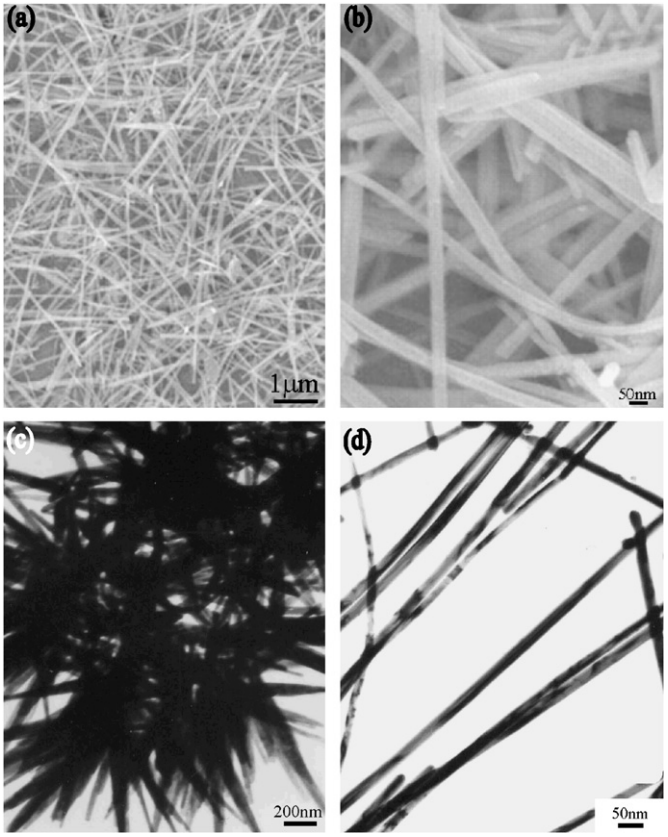

Fig. 2. SEM and TEM images of the Cu_3SbS_3 nanowires.

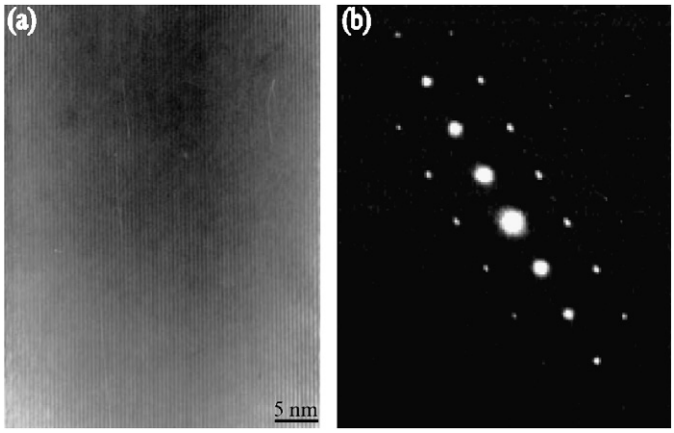

Fig. 3. HRTEM and SAED images of the single Cu_3SbS_3 nanowires.

Fig. 2(d) indicates that the Cu_3SbS_3 nanowires with a diameter of about 30 nm and a length up to hundreds of nanometers are straight and smooth. The morphology and nanostructure of the Cu_3SbS_3 nanowires were further investigated with HRTEM and SAED. The HRTEM image of a single Cu_3SbS_3 nanowire is given in Fig. 3(a). Seen from this image, the lattice fringes of the Cu_3SbS_3 are clear and uniform, additionally confirmed that these single-crystalline Cu_3SbS_3 nanowires are of high quality. The SAED pattern (Fig. 3(b)) taken from a single nanowire, indicates that the Cu_3SbS_3 nanowires are good single crystalline.

The quality and composition of the product were characterized by XPS. The XPS spectra of Cu_3SbS_3 nanowires are shown in Fig. 4. Seen from Fig. 4(a), the full spectrum of the product indicates that no obvious impurities besides copper, antimony, and sulfur

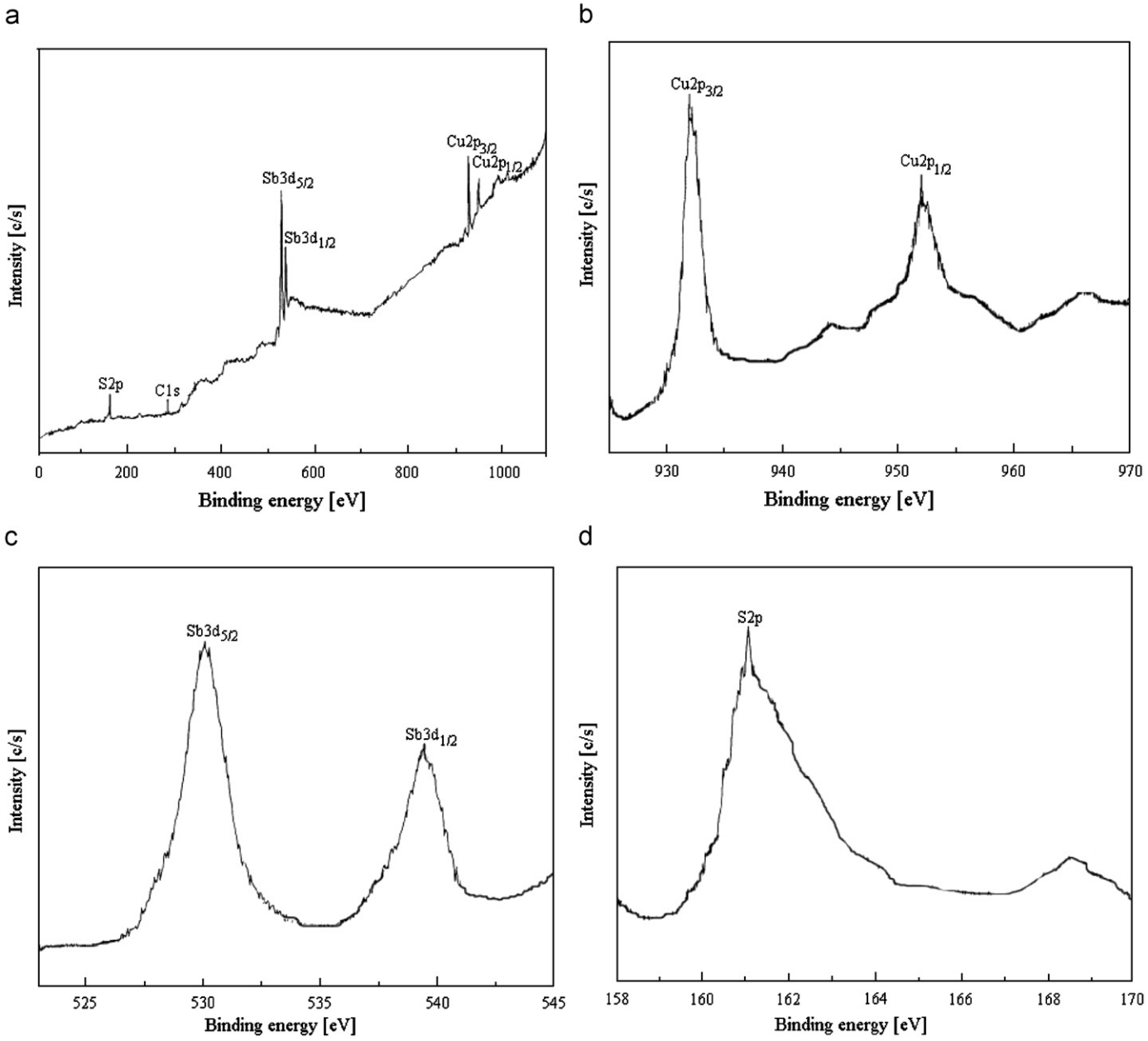

Fig. 4. XPS analyses of the as-prepared nanocrystalline Cu_3SbS_3 nanowires.

elements. The Cu2p core-level spectrum (Fig. 4(b)) shows that the observed value of the binding energy for $Cu2p_{3/2}$ (932.15 eV) is close to the reported value of Cu^+ [18], and there is no $Cu2p_{3/2}$ satellite peak at about 942 eV [19] attributed to Cu^{2+}. In addition, another binding energy for $Cu2p_{1/2}$ (951.56 eV) is also attributed to $Cu^{1\pm}$. The Sb3d core-level spectrum (Fig. 4(c)) reveals the binding energy for $Sb3d_{5/2}$ (529.80 eV) and $Sn3d_{3/2}$ (539.25 eV) are in good agreement with the values of Sb^{3+}. The S2p core-level spectrum (Fig. 4(d)) indicates values of the binding energy for $S2p_{3/2}$ (161.50 eV) is consistent with those values in Ref. [20]. Besides, minor features are assigned to carbon (C 1s, 284.8 eV) and oxygen (O 1s, 531.8 eV), which are from the absorbed gaseous molecules. Hence, the XPS analysis shows the normal valence states for Cu_3SbS_3 are $Cu_3^{1+}Sb^{3+}S_3^{2-}$.

The results of energy-dispersive spectra (EDS) give a rough atomic ratio Cu/Sb/S of 3:1:3, which is in good agreement with the XPS results.

Fig. 5 shows the room temperature optical emission spectrum of Cu_3SbS_3 nanowires. When exciting with 234 nm Xe light source, the Cu_3SbS_3 nanowires show one emission band centered at 364 nm. The observed emission band can be assigned to the emission from the recombination of electrons and holes in trapped surface states located in the "forbidden" region of the bandgap [21].

The optical characteristics were measured and show a plot of $\alpha h\nu$ against $h\nu$ in Fig. 6, where $h\nu$ was the photon energy. The optical energy gap, E_{opt}, was obtained by extrapolating the absorption edge line to the abscissa of $h\nu$ according to the standard Tauc's plot technique, and the value of E_{opt} is about 2.95 eV. The transition is indirect and consistent with the electronic structure calculations and the analysis of diffuse reflectance spectrum of K_2CuSbS_3, which led to indirect bandgap energy of 2.2 eV [22]. The present electronic structure calculations underestimated the bandgap energy of Cu_3SbS_3, probably can be

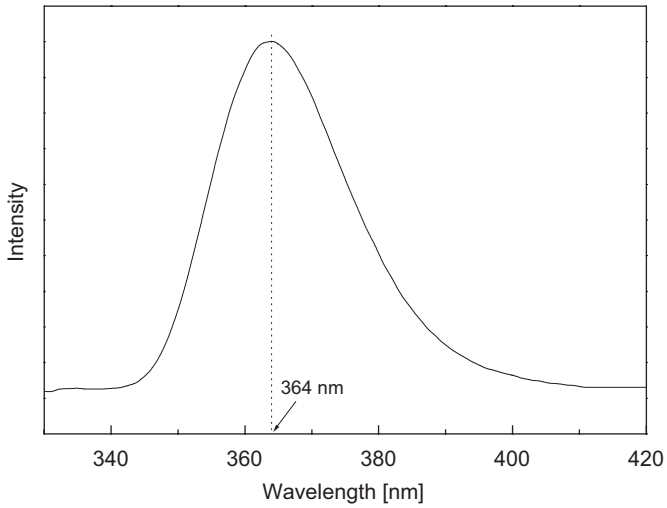

Fig. 5. Room temperature emission spectrum of the as-prepared Cu_3SbS_3 nanowires.

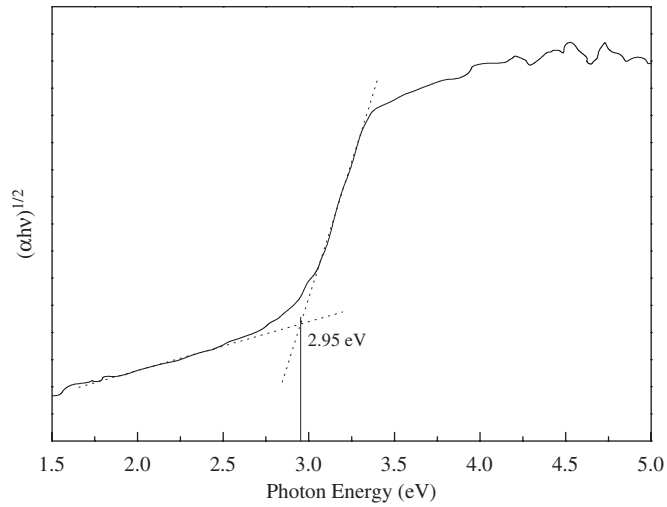

Fig. 6. The bandgap of the Cu_3SbS_3 nanowires prepared at 160 °C.

attributed to the local-density approximation [23]. Both the local-density approximation and the generalized gradient approximation exchange-correlation potential improperly account for strongly correlated 3*d* electrons. However, the topology of the band structure is correctly provided by the local-density approximation.

In the whole reaction process, ethylenediamine played an important role in the formation of pure Cu_3SbS_3 nanowires [24,25]. Being a N-chelating ligand, ethylenediamine could slowly dissolve CuCl to form corresponding complexes, at relatively low temperature. One of the evidences is that the solution color changes from transparent to light then to dark blue when CuCl was added into ethylenediamine. In addition, being a reducing solvent and having stronger reductibility under the solvothermal conditions, ethylenediamine could reduce Cu^+ and Sb^+ to active atomic Cu and Sb. When CuCl dissolved in ethylenediamine, the stable complexes were rapidly formed, but the stability of complexes decreased with the increasing reaction temperature, thus more and more Cu^+ could be released and reduced by ethylenediamine to atomic Cu. Meanwhile, Sb^{3+} was also reduced to atomic Sb. Under the solvothermal conditions, these newborn atoms were rather active; subsequently they combined with elemental sulfur, which was dissolved in ethylenediamine and formed nanocrystalline Cu_3SbS_3. The whole process can be described by the following reactions:

$$CuCl \xrightarrow{en} Cu(en)_x^+ \xrightarrow{\Delta} Cu^+ \xrightarrow[\Delta]{en} Cu$$

$$SbCl_3 \xrightarrow{en} Sb(en)_y^{3+} \xrightarrow{\Delta} Sb^{3+} \xrightarrow[\Delta]{en} Sb$$

$$24Cu + 8Sb + 3S_8 \Rightarrow 8Cu_3SbS_3$$

In our approach, suitable reaction temperature and time not only brought about the above reactions, but also controlled the crystallinity and grain size of the final product. When the reaction temperature was lower than 100 °C, complexes were rather stable and it was difficult to release free metallic ions; meanwhile, the reductibility of ethylenediamine was weak, so only a trace of elemental antimony appeared in the final products. The incomplete reactions which may lead by lower temperature or shorter time, decreased the yield and the crystallinity of the desired products that with some impurities, such as Sb_2S_3, elemental Cu and Sb. In this case, these newborn metal atoms were not active enough to completely combine with elemental sulfur dissolved in ethylenediamine, so pure Cu_3SbS_3 could not be obtained. On the other hand, as the rapid decomposition of complexes and the stronger reductibility of ethylenediamine at higher temperature, the metal atoms would rapidly produce and keep rather active, they rapidly combined with elemental sulfur. Thus, as it was difficult to control the nucleation and the growth of Cu_3SbS_3 crystallites, the resulting crystalline grain grew larger at higher temperature or for longer time as it was difficult to obtain nanocrystals. All the facts show that, at suitable temperature, only when the decomposition velocity of complexes could be controlled and the reductibility of ethylenediamine was strong enough, newborn metallic atoms would be easily produced and keep active enough. Thus the metallic atoms would steadily combine with elemental sulfur, the nucleation and the growth of crystalline Cu_3SbS_3 could be controlled and pure nanocrystallites could be easily obtained. In our report, the optimum conditions for preparing nanocrystals were at 160 °C for 24 h.

4. Conclusion

Cu_3SbS_3 nanowires with orthorhombic structure was successfully obtained through mild solvothermal routes at 150, 160, and 170 °C for 24 h, based on reactions between CuCl, $SbCl_3$ and elemental sulfur in ethylenediamine. Being a reaction medium and an excellent reducing ligand, ethylenediamine directly took part in the whole reaction processes. And at proper temperature and time, reactions could steadily be proceeded, the nucleation and the growth were easily controlled, and the nanocrystalline Cu_3SbS_3 formed homogeneously. With reaction media selected carefully, other nanocrystalline materials with similar compositions were expected to be obtained under similar solvothermal conditions.

References

[1] F.J. Disalvo, Science 247 (1991) 649.
[2] G.H. Yue, P.X. Yan, et al., Appl. Phys. Lett. 87 (2005) 262505.
[3] M. Onoda, X.A. Chen, A. Sato, H. Wada, Mater. Res. Bull. 35 (2000) 563.
[4] G. Marcano, L.M. de Chalbaud, C. Rincon, G. Sanchez Perez, Mater. Lett. 90 (2002) 1847.
[5] G.H. Yue, P.X. Yan, et al., J. Appl. Phys. 100 (2006) 124313.
[6] G.H. Yue, P.X. Yan, et al., Electrochem. Solid State Lett. 10 (2007).
[7] M.G. Kanatzidis, J.H. Chou, J. Solid State Chem. 127 (1996) 186.
[8] K. Chondroudis, M.G. Kanatzidis, Inorg. Chem. 37 (1998) 2098.
[9] A. Henglein, Top. Curr. Chem. 147 (1989) 113.

[10] L.A. Brus, J. Phys. Chem. 90 (1986) 2555.
[11] R.P. Andres, R.S. Averback, W.L. Brown, et al., Mater. Res. 4 (1989) 704.
[12] A. Stein, S.W. Keller, T.E. Mallouk, Science 259 (1993) 1558.
[13] P.T. Wood, W.T. Pennington, J.W. Kolis, J. Chem. Soc. Chem. Commun. (1993) 235.
[14] D. Chen, G.Z. Shen, K.B. Tang, et al., Mater. Res. Bull. 38 (2003) 509.
[15] G.H. Yue, P.X. Yan, et al., J. Crystal Growth 293 (2006) 428.
[16] G.H. Yue, P.X. Yan, et al., Appl. Phys. A 84 (2006) 409.
[17] G.H. Yue, P.X. Yan, et al., J. Crystal Growth 294 (2006) 385.
[18] C.D. Wagner, W.M. Riggs, L.E. Davis, J.F. Molder, G.E. Muilenberg (Eds.), Handbook of XPS, Perkin-Elmer Corporation, Eden Prairie, MN, 1979.
[19] L.D. Partain, R.A. Schnerder, L.F. Donaghey, P.S. Meleod, J. Appl. Phys. 57 (1985) 5056.
[20] J.Q. Hu, B. Deng, K.B. Tang, C.R. Wang, Y.T. Qian, J. Mater. Res. 12 (2001) 3411.
[21] J. Cizeron, M.P. Pileni, J. Phys. Chem. B 101 (1997) 8887.
[22] B. Deng, G.H. Chan, D.E. Ellis, J. Solid State Chem. 178 (2005) 3169.
[23] M.S. Hybertsen, S.G. Louie, Phys. Rev. B 34 (1986) 5390.
[24] X.Y. Chen, X. Wang, C.H. An, J.W. Liua, Y.T. Qian, J. Crystal Growth 256 (2003) 368.
[25] H.L. Su, Y. Xie, S.K. Wan, B. Li, Y.T. Qian, Solid State Ionics 123 (1999) 319.